Effect of carbide size in hardfacing on abrasive wear

R. Chotěborský[1], P. Hrabě[1], M. Müller[1], R. Válek[2], J. Savková[3], M. Jirka[1]

[1]*Department of Material Science and Manufacturing Technology, Faculty of Engineering, Czech University of Life Sciences Prague, Prague, Czech Republic*
[2]*SVUM Ltd., Czech Republic*
[3]*New Technologies Research Centre in Westbohemian Region – NTC, University of West Bohemia, Pilsen, Czech Republic*

Abstract: Abrasive wear of high alloyed overlay materials with high contents of carbide phases of M_7C_3 depends on the sizes of the carbide particles and on their distribution in an overlay. This work is focused on the study of the carbide particles size effect on abrasive wear. The size of carbide particles of M_7C_3 type, their distribution (part) in the matrix and their effect on abrasive wear were measured. Hardness in single layers, as well as microhardness of the matrix and of carbide particles, were also measured. The abrasive wear resistance was measured using the pin-on-disk machine with bonded abrasive particles. For the study of the chemical composition, the scanning electron microscopy with energy dispersive X-ray analysis (EDX) was used.

Keywords: abrasive wear; weld deposition; hardness; pin-on-disk; carbides

The weld deposition of hardfacing alloys is commonly employed in industry to increase the service life of components subjected to abrasive wear (Gregory 1980; Gulenc & Kahraman 2003).

Surface coating is employed to increase the wear and corrosion resistance of steel (Eroglu & Ozdemir 2002). Surface treatments may improve the surface resistance to corrosion, impact, or abrasive wear. However, no single surface treatment will give maximum resistance to all these types of deterioration at the same time (Althouse *el al*. 1992).

It is known that the abrasive wear rate can often be reduced by the application of hard materials. To characterize the abrasive wear behaviour, the transition from low wear to high wear with increasing hardness of the abrasive is very instructive (Habig 1989; Chotěborský *et al*. 2007).

Hardfacing is a surface treatment aimed at improving the surface properties of metals, in which an overlay after welding, having excellent resistance to wear and oxidation, is deposited onto the surface of a substrate. It is mainly applied to parts exposed to various wear environments in order to protect them and to extend their life (Kim *et al*. 2003).

Iron-based alloys with substantial concentrations of chromium and carbon and a microstructure containing a large volume fraction of hard carbides are often used for cladding the surfaces of components subjected to abrasion, largely because of their good wear resistance properties attained at a low cost. The alloys are often deposited by arc welding, in which case the cooling rates can be sufficiently large to give nonequilibrium microstructure of M_7C_3 carbides grow as rods and blades with their long axis parallel to the flow direction in the mold (Dogan & Hawk 1995). The application of these Fe-Cr-C alloys to wear resistant parts exposed to considerable external impact is limited, because they contain large particles of brittle chromium carbides (Lee *et al*. 1996).

MATERIALS

The substrate material was steel ČSN EN S235JR with the dimensions of 250 × 100 × 25 mm. The com-

Supported by the Czech Science Foundation, Grant No. 101/07/P124, and by the Internal Grant Agency of the Czech University of Life Sciences in Prague, Faculty of Engineering, Project No. 31140/1312/313113.

Table 1. Chemical composition of the electrode according to the manufactur's data (weight %)

	C	Cr	Mo	V	W	Nb	Fe
Electrode	4.4	23.5	6.5	1.5	2.2	5.5	balance

mercial hardfacing and buffer consumables, in the form of coated electrodes, were used according to the recommendation of the electrode manufacturer. Chemical composition of the electrode is shown in Table 1.

Welding conditions for hardfacing deposits

The hardfacing electrodes were deposited on the plate without preheating in the flat position using the manual metal arc welding method. Before welding, the electrodes were dried at 100°C for 2 h. On completion the weld deposits, each test piece was allowed to cool in air. The welding parameters of the electrodes are given in Table 2.

Table 2. Welding conditions

Electrode diameter (mm)	3.2
Arc voltage (V)	27
Welding current (A)	150
Electrode polarity	positive
Preheating	no
Electrode angle	10°
Deposition rate (kg/h)	14
Number of layers	2

Chemical composition, metallography, and hardness test

The chemical composition (Table 3) was determined on the overlay surface of the specimen using Glow Discharge Optical Emission Spectroscopy (GDOES) (Vnouček 2001). The hardfacing deposited plates were sectioned for chemical analysis, metallographic specimens (20 × 20 × 25 mm), and also for wear test specimen (25 × 25 × 25 mm) using the high speed SiC cutter with cooling. The specimen prepared from the plate is shown in Figure 1.

Metallography test specimens were then ground using a belt grinder and grit papers and finally polished with Al_2O_3 powder suspension, cleaned with acetone, and dried. The polished metallography specimens were etched with Vilella-Bains reagent and the microstructures were observed using an optical microscope.

The specimens were evaluated using scanning electron microscopy enabling the determination of the chemical composition. Some test specimens were selected to evaluate the worn surfaces by means of scanning electron microscopy, in an attempt to provide a better understanding of the wear mechanism.

The overall bulk hardness of the hardfaced layer and microhardness of the matrix and carbide phase were measured using the Vickers hardness tester under 30 kg, respectively 0.1 kg load weight for microhardness. The overlay hardness and the matrix microhardness were measured across the surfacing direction. Chemical analysis was carried out according to Energy dispersive X-ray analysis (EDX) on the side of the specimen in lines of 1 mm length in the direction of surfacing. These lines were placed in distances of every 0.5 mm from the surface to the basic material.

Size of carbide particles

The carbide phase geometry and the matrix structure were evaluated using the methods of optical metallography. The phases fraction was determined using the digital image analysis. The carbide phase size was measured according to the carbide surface of the metallographic cut. The form of the carbide cut can be approximated by an ellipse. The surfaces of single carbides A were calculated using the lengths of the principal axis d_{max} and the minor axis d_{min} according to the formula:

$$A = \frac{\pi \times d_{max} \times d_{min}}{4} \quad (1)$$

Table 3. Chemical composition of the overlay (weight %)

Element	C	Si	Cr	Mn	Mo	Nb	W	V	Fe
Overlay	4.26	1.09	21.69	0.21	4.63	5.92	1.00	1.55	balance

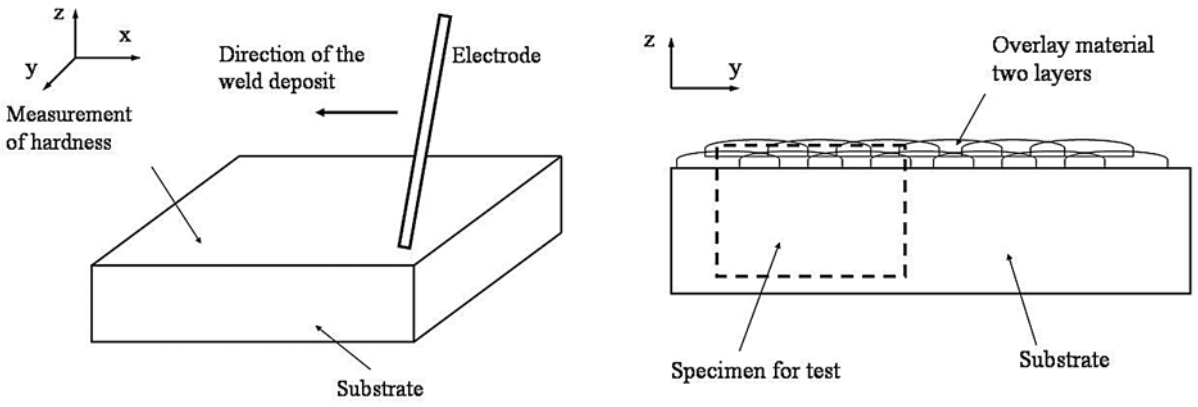

Figure 1. Diagrammatic representation of surfacing, specimen cut-out, and hardness measurement

The formula of the probability density of logarithmic-normal distribution is:

$$f(x) = \frac{1}{x \times \sigma \times \sqrt{2\pi}} \times e^{-\frac{(\ln x - \mu)^2}{2\sigma^2}} \quad (2)$$

where:
x – carbide surface
μ – mean of $\ln x$
σ – standard deviation of $\ln x$

In order to overcome the shortcomings of the preliminary analysis, a more detailed assessment was performed using the image analysis. According to Figure 2, the parameters d_{max}, d_{min}, and the angle α can be directly measured. The angle β can be determined from Eq. (3) (Dlouhý & Eggler 1992).

$$\beta = \arcsin\left(\frac{d_{min}}{d_{max}}\right) \quad (3)$$

Abrasive wear test

Before the abrasive wear test, all specimens were cleaned with acetone and then weighed using the mechanical balance of an accuracy of ± 0.05 mg. The laboratory tests of the relative wear resistance were carried out using the pin-on-disk machine with the abrasive cloth (Al_2O_3, 1800–2300 HV, grit 120) according to ČSN 01 5084. The pin-on-disk machines are used most often. The simplicity and reliability are their advantages. The results variance is relatively small. The variable quality of the abrasive cloth must be continuously compensated by the use of etalons. The pin-on-disk testing machine (Figure 3) consists of a uniform rotating disk whereon the abrasive cloth is fixed. The specimen tested is fixed in the holder and pressed against the abrasive cloth with the weight of 2.35 kg. The screw makes the radial feed of the specimen possible. The limit switch stops the test. During the test, the specimen moves from the outer edge to the centre of the abrasive cloth and a part of the specimen comes in contact with the unused abrasive cloth, namely 1.25 mm/1 revolution.

The wear resistance was tested in various overlay zones as long as the limit stage was reached. The limit stage was reached at the time when the tested

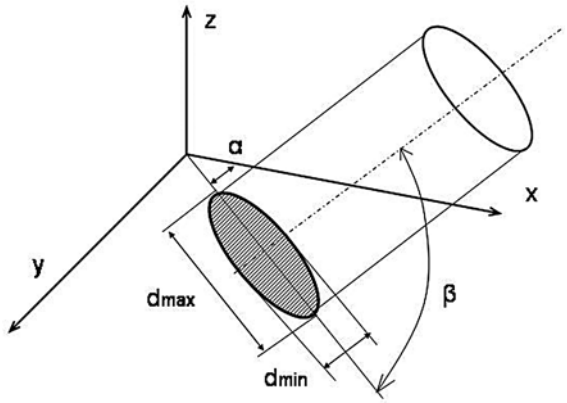

Figure 2. Schematic illustration of the orientation of a carbide in space, definition of the angles α and β

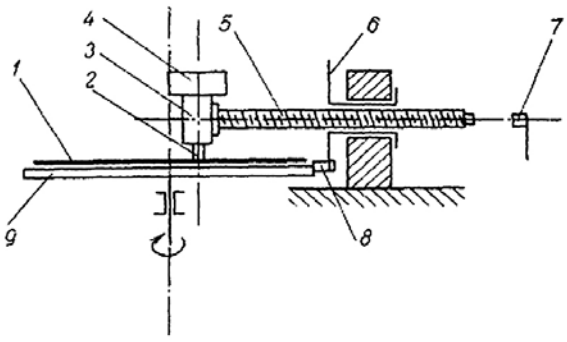

Figure 3. Operating principle of the pin-on-disk testing machine: 1 – abrasive cloth, 2 – specimen, 3 – holder, 4 – weight, 5 – screw, 6 – nut with cogs, 7 – limit switch, 8 – pin, 9 – horizontal plate

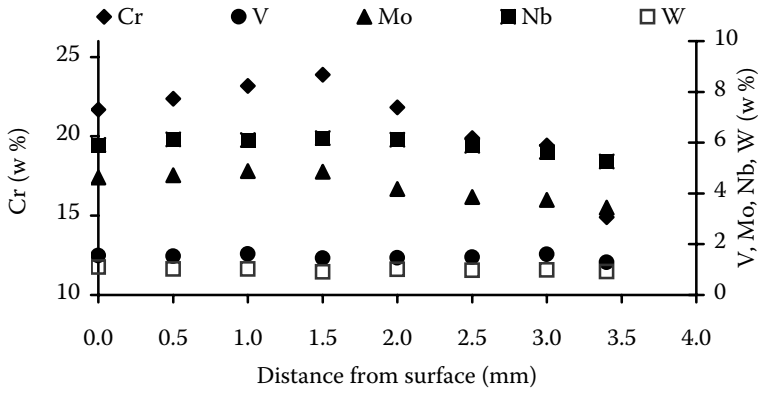

Figure 4. Overlay composition determined by means of EDX

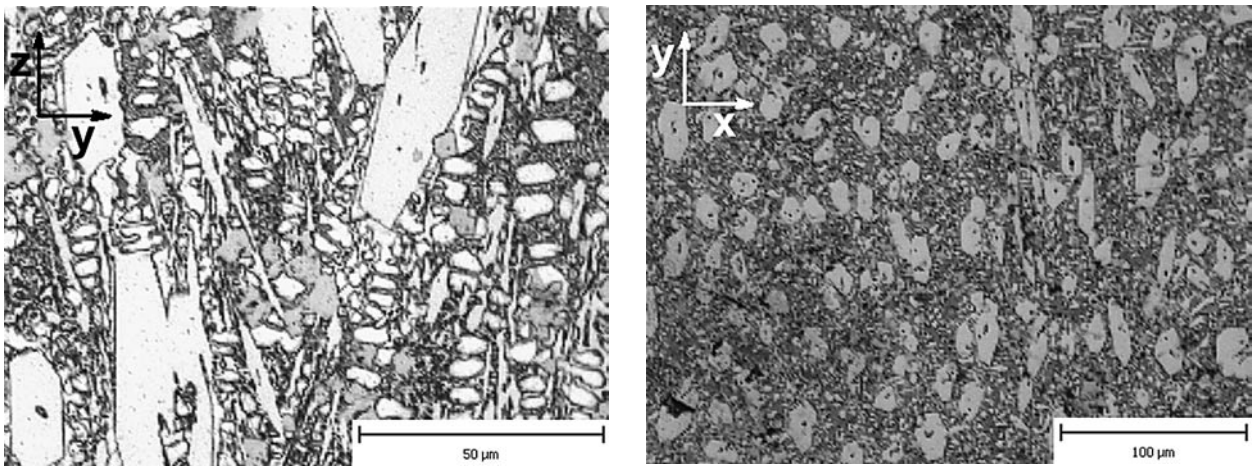

Figure 5. Microstructures of longitudinal and cross sections with regard to the surfacing direction in the distance of 1.4 mm from the surface

surface contained less than 90% of the second layer overlay material.

$$\Psi_w = \frac{m}{l} \quad (4)$$

where:
Ψ_w – wear rate (mg/m)
m – mass defect
l – distance done (41.5 m)

RESULTS

Overlay microstructure characterization and chemical composition

The chemical composition of the overlay is presented in Table 3, the overlay composition in various distances from the surface in Figure 4, the longitudinal and normal overlay microstructures with

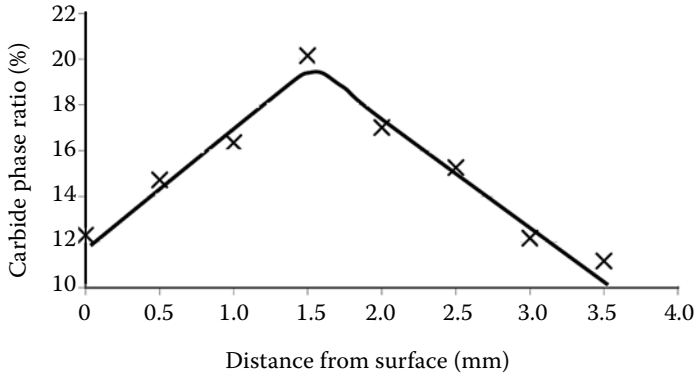

Figure 6. Carbide phase proportions (M_7C_3) in various distances from the surface

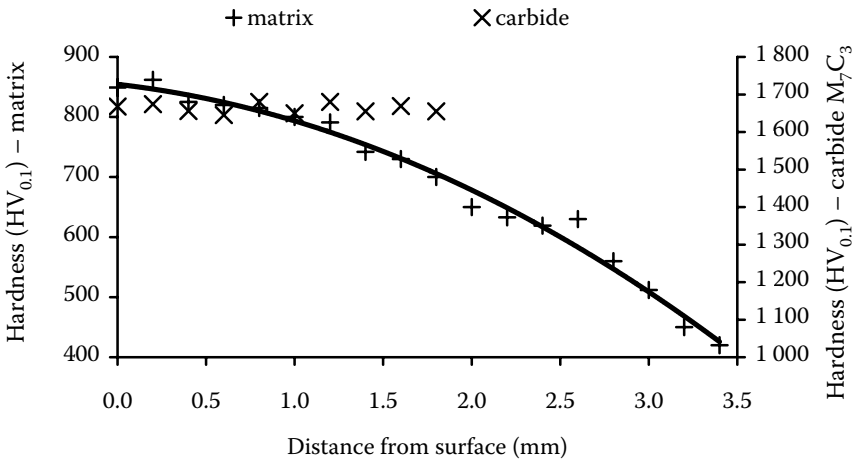

Figure 7. Relation between matrix and carbides hardness and distance from surface

Table 4. Chemical composition of the measured object (weight %)

Place	C	O	Si	Mo	V	Cr	Mn	Fe	W	Nb
1	34.11	0.24	0.08	0.5	1.61	26.99	0	33.82	0.69	1.97
2	30.66	0.92	0.05	0.54	1.69	28.51	0	35.74	0.64	1.25
3	36.56	0.05	0.05	5.50	1.28	1.47	0.08	1.73	0.77	52.51
4	1.26	0	0.62	0.38	0.30	6.65	0.53	89.11	0.69	0.46

regard to the surfacing direction in the distance from the surface of 1.4 mm in Figure 5, and the carbide phases ratio in various distances from the surface in Figure 6.

By the use of optical metallography, it was determined that in the overlay layer Cr and Nb carbides occur. The hardness of Cr carbides is presented in Figure 7. Their ratio in various distances from the surface is shown in Figure 6. The hardness of Nb carbides $HV_{0.05}$ was 2350 to 2500 and their proportion was 3% in all distances.

Aside from the optical metallography, the method of back reflected electrons and EDX were used for the determination of the chemical composition of the phases occurring in the overlay. Figure 8 shows the structure using BSE (back scattered electron). Table 4 presents the chemical composition of the objects measured. The carbon content is taken into consideration.

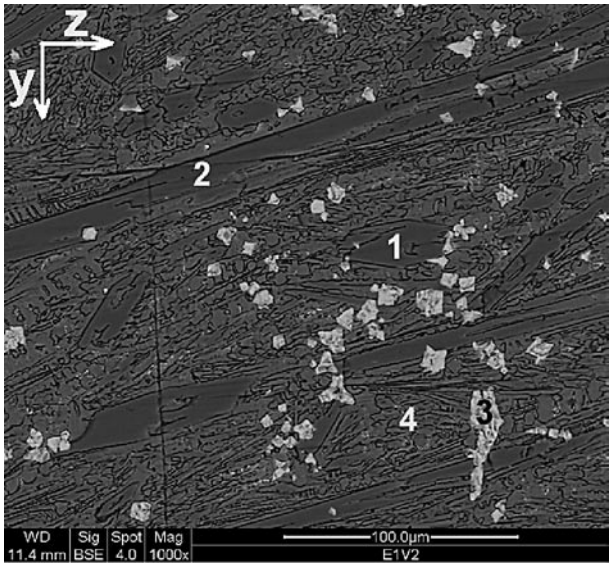

Figure 8. Structure of the overlay in depth of 2.5 mm determined by SEM (BSE) method

Carbide phase size and its orientation

The size of carbide particles (surface *A*) was calculated according to the formula (1). The dependence on the position in the overlay is shown in Figure 9. For the determination of the carbides length, the cutout of 0.5 mm height was used. Therefore, in Figure 10 the average length of carbides is presented in distances from the surface 0–0.5 mm, 0.5–1 mm etc. The course of the particles size corresponds to the normal heat flow during the overlay cooling.

Hardness and wear test

The hardness ($HV_{0.1}$) of the overlay matrix in the dependence on the distance from the surface

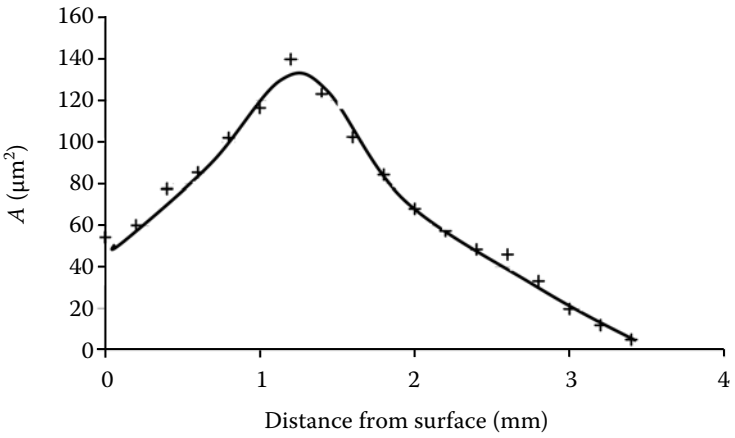

Figure 9. Relation between carbide particles size (surface *A*) and distance from surface

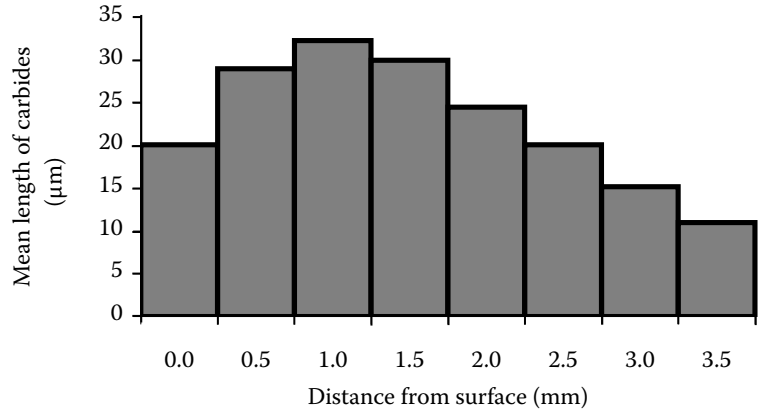

Figure 10. Relation between carbides length and distance from surface

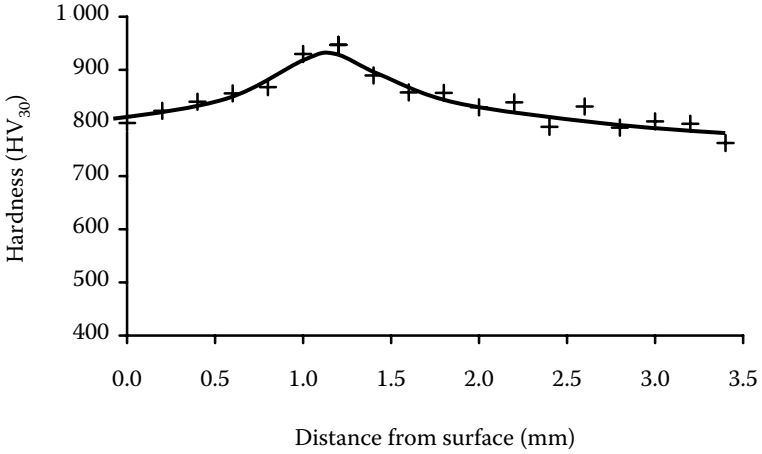

Figure 11. Relation between overlay hardness and distance from surface

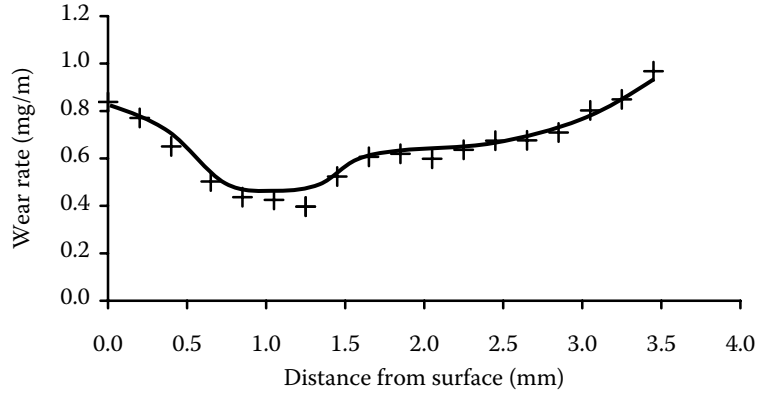

Figure 12. Relation between wear rate and distance from surface

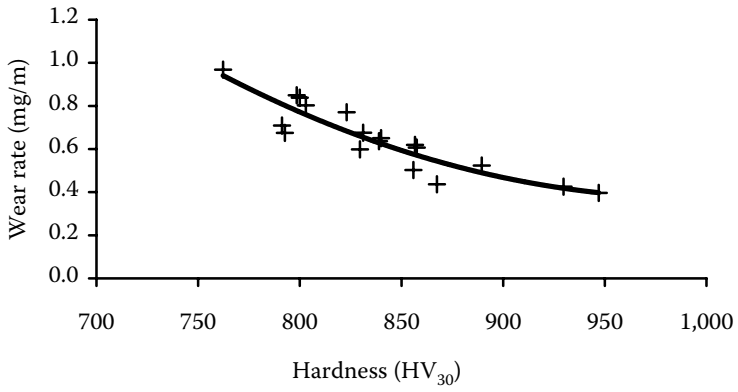

Figure 13. Relation between wear rate and overlay total hardness

is shown in Figure 7. The hardness of the matrix decreases in the direction to the substrate. This decrease corresponds to the overlay and substrate cooling conditions of natural slow cooling after surfacing. The average hardness ($HV_{0.1}$) of the carbides measured was almost identical and was measured only to the depth of 1.8 mm because, over this depth, the carbides size was smaller than the microhardness measuring $HV_{0.1}$ allowed. For lower loads, the indenture diagonals measuring was unreal.

The overlay total hardness (HV_{30}) in the dependence on the distance from the surface is shown in Figure 11. The total hardness is influenced not only by the matrix and carbides hardness, but also by the carbide phase surface of the overlay concrete cut. It is possible to say than the total hardness corresponds to the amount and size of carbide particles.

The relation between the wear rate and the distance from the surface is shown in Figure 12. The wear rate is proportional to the total overlay properties (structure, hardness, toughness etc.), which consist of matrix properties, size, and rate of carbide particles.

The relation between the wear rate and the overlay total hardness is presented in Figure 13.

The scanning electron microscope micrographs of worn surface are shown in Figure 16.

DISCUSSION

Microstructure, hardness and volume fraction of carbide phase

The overlay microstructure corresponds to the system Fe-Cr-C-M. In the structure, the hypereutectic carbides configurations occur. This is perceptible in Figure 5. The carbides size was variable in the dependence on the distance from the surface (Figures 7 and 8). The carbide phase proportion corresponds to the determined chemical composition, therefore

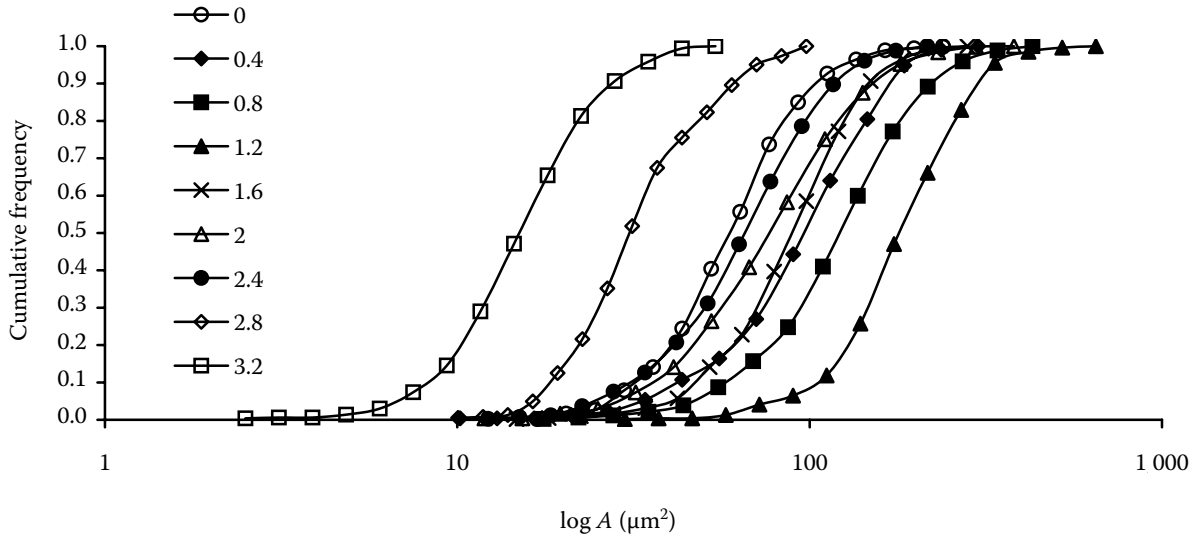

Figure 14. Relation between cumulative frequency and size of carbide at various distances from surface

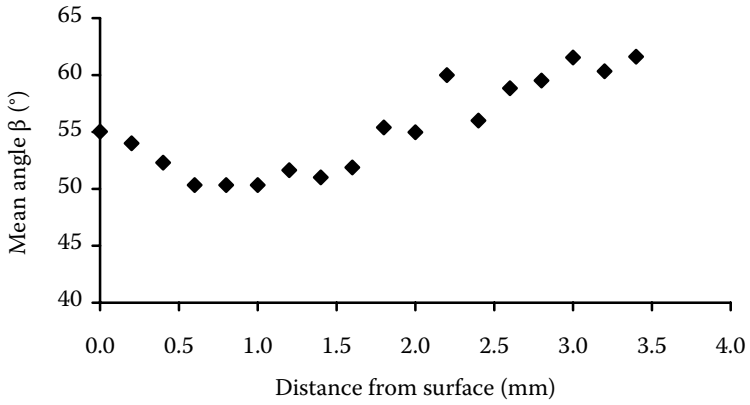

Figure 15. Relation between median of angle β and distance from surface

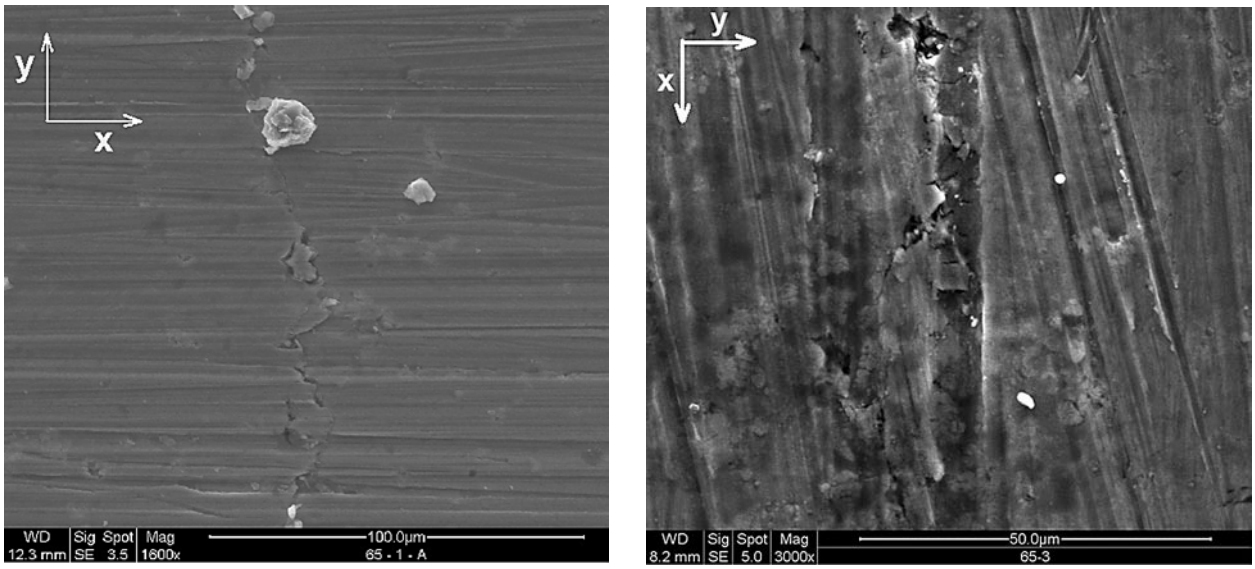

Figure 16. Scanning electron microscope micrographs of worn surface, low magnification, high magnification

the course of the carbide particles amount (Figure 14) accords with the chemical composition.

In the matrix, the carbide particles are partly influenced and determined by the position of carbides in the system. Therefore, the angle β (Figure 15) was observed. The angle β is minimal in the depth range of 0.5–1.5 mm. In the projection, this position increases the carbide surface *A*. The range of minimal angles β corresponds to the range of maximal surface *A* of carbide particles.

The overlay hardness was maximal in the depth of 1.2 mm. This maximum does not correspond to the maximal proportion of the carbide particles in the matrix. However, at measuring the microhardness of carbide particles and the matrix surrounding them, it is perceptible that with the distance from

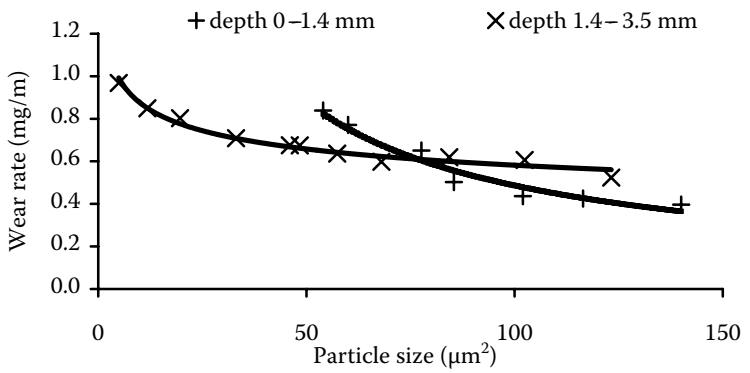

Figure 17. Wear rate related to carbide particles size

the surface, the hardness of the matrix expressively decreases.

Abrasive wear

At the size of carbides *A* from 30 to 140 μm^2 the groove width was smaller than the carbide size. At the size of carbides *A* of 20 to 30 μm^2, the groove width was approximately the same. At the size of carbides *A* less than 20 μm^2, the groove width was larger than the carbides size. In the distance from the surface from 0.8 to 1.4 mm, more than 95% carbides were larger than 30 μm^2, therefore the measuring results showed approximately the same abrasive wear resistance. With the increasing part of carbides of the size *A* less than 30 μm^2, the abrasive wear resistance decreases.

The minimum of the abrasive wear rate was determined in the overlay depth of 0.8–1.4 mm. This range corresponds to the maximal overlay hardness, to the maximal carbides surfaces *A*, and to the maximal proportion of the latter in the matrix. With regard to the fact that the occurrence of hypereutectic carbide particles influences mostly the abrasive wear resistance, the relation between the abrasive resistance and carbides surfaces *A* was determined. This relation is shown in Figure 16. The variable matrix hardness was respected and therefore, the interlay was divided into the carbide surfaces *A* from 0 mm to 1.4 mm and those from 1.4 mm to 3.4 mm (Figure 17).

CONCLUSIONS

– The size of hypereutectic carbides corresponds to the heat flow during the surfacing.
– The angle β influences the value of hypereutectic carbides size *A*.
– The course of abrasive wear resistance depends on the position in the overlay and corresponds to the courses of total hardness and to the hypereutectic carbides size *A*.
– The maximum abrasive wear resistance is in the range of the maximum hypereutectic carbides size *A*.
– The abrasive wear resistance decreases with the decreasing hypereutectic carbides size *A* but is influenced by the matrix hardness as well.

References

Althouse A.D., Turnquist C.H., Bowditch W.A., Bodwitch K.E. (1992): Metal surfacing. In: Modern Welding: 563–565.

Dlouhý A., Eggler G. (1992): A quantitative metallographic study of a short fibre reinforced aluminum alloy. Praktische Metallographie, **30**: 172–185.

Dogan O.N., Hawk J.A. (1995): Effect of carbide orientation on abrasion of high Cr white cast iron. Wear, **189**: 136–142.

Chotěborský R., Hrabě P., Müller M. (2007): Properties of martensitic overlays. Research in Agricultural Engineering, **53**: 116–120.

Eroglu M., Ozdemir N. (2002): Tungsten-inert gas surface alloying of a low-carbon steel. Surface and Coatings Technology, **154:** 209–217.

Gregory E.N. (1980): Surfacing by welding – Alloys, processes, coatings and materials selection. Metal Construction, **12**: 685–690.

Gulenc B., Kahraman N. (2003): Wear behaviour of bulldozer rollers welded using a submerged arc welding process. Materials and Design, **24**: 537–542.

Habig K.H. (1989): Wear behaviour of surface coatings on steel. Tribology International, **22**: 65–73.

Kenneth G., Budinski K.G. (1988): Surface Engineering for Wear Resistance. Prentice-Hall, Inc., New York.

Kim C.K., Lee S., Jung J.Y., Ahn S. (2003): Effects of complex carbide fraction on high-temperature wear properties of hardfacing alloys reinforced with complex carbides. Materials Science and Engineering A, **349**: 1–11.

Lee S., Choo S.H., Baek E.R., Ahn S., Kim N.J. (1996): Correlation of microstructure and fracture toughness in high-chromium white iron hardfacing alloys. Metallurgical and Materials Transactions A, **27A**: 3881–3891.

Vnouček M. (2001): Surface effects with GDOES. [Ph.D. Thesis.] University of West Bohemia, Pilsen. (in Czech)

Received for publication February 5, 2009
Accepted after corrections May 21, 2009

Abstrakt

Chotěborský R., Hrabě P., Müller M., Válek R., Savková J., Jirka M. (2009): **Vliv velikosti karbidu v tvrdonávaru na abrazívní opotřebení**. Res. Agr. Eng., **55**: 149–158.

Abrazivní opotřebení vysokolegovaných návarových materiálů s vysokým obsahem karbidické fáze M_7C_3 závisí na velikosti karbidů a jejich distribuci v návarové vrstvě. Práce byla zaměřena na studium vlivu velikosti karbidu na

abrazívní opotřebení. Byla měřena velikost karbidu a její distribuce v návarové vrstvě. Taktéž byla hodnocena tvrdost a mikrotvrdost jak karbidu tak i matrice návaru. Abrazívní opotřebení bylo měřeno na přístroji typu pin-on-disk s vázaným abrazivem. Pro studium bylo využito metod chemické analýzy a elektronové mikroskopie s energiově disperzní rentgenovou analýzou EDX.

Klíčová slova: abrazívní opotřebení; návar; tvrdost; pin-on-disk; karbidy

Corresponding author:

Ing. Rostislav Chotěborský, Ph.D., Česká zemědělská univerzita v Praze, Technická fakulta,
katedra materiálu a strojírenské technologie, Kamýcká 129, 165 21 Praha 6-Suchdol, Česká Republika
tel.: + 420 224 383 274, fax: + 420 234 381 828, e-mail: choteborsky@tf.czu.cz